The Cohesive-Adhesive Balances in Dry Powder Inhaler Formulations I: Direct Quantification by Atomic Force Microscopy

Philippe Begat,[1] David A.V. Morton,[2] John N. Staniforth,[2] and Robert Price[1,3]

Received February 20, 2004; accepted May 18, 2004

Purpose. To obtain a quantitative assessment of the cohesive and adhesive force balance within dry powder inhaler formulations.
Methods. The atomic force microscope (AFM) colloid probe technique was used to measure the adhesive and cohesive force characteristics of dry powder systems containing an active component (budesonide, salbutamol sulphate) and α-lactose monohydrate. To minimize the variations in contact area between colloid probe and substrates, nanometer smooth crystal surfaces of the drugs and the excipient were prepared.
Results. The uniformity in contact area allowed accurate and reproducible force measurements. Cohesive-adhesive balance (CAB) graphs were developed to allow direct comparison of the interaction forces occurring in model carrier-based formulations. A salbutamol sulphate-lactose system revealed a significant tendency for the two materials to adhere, suggesting a propensity for the powder to form a homogenous blend. In contrast, the budesonide-lactose system exhibited strong cohesive properties suggesting that the formulation may exhibit poor blend homogeneity and potential for segregation upon processing and handling.
Conclusions. The novel approach provides a fundamental insight into the cohesive-adhesive balances in dry powder formulations and further understanding of powder behavior.

KEY WORDS: AFM; DPI; lactose; particle adhesion; formulation.

INTRODUCTION

The adhesion between a micrometer-sized particle and a solid surface is a result of a complex combination of physical forces. These include the ubiquitous van der Waals forces, as well as possible influences from electrostatic and capillary forces (1). The contribution of each of these forces to the overall adhesion is dependant on various factors, including the physical properties of the contiguous surfaces [surface and interfacial free energies (2,3), mechanical properties (4), and contact area, as well as environmental conditions (temperature and relative humidity (5–7)]. However, direct characterization of the specific influence of these individual forces and their dependence on physico-mechanical and environmental conditions are difficult to discern. Well-established techniques for measuring particle adhesion include centrifugal particle detachment, fluid dynamic and vibration methods (8–10). These techniques provide quantitative information concerning the integrated effect of physical and environmental variations on particle adhesion. They are, however, severely limited when the properties that influence the adhesion of an individual particle and a substrate surface are required. With the advent of the atomic force microscope (AFM) and the development of the colloid probe technique, quantification of the total interaction force between an individual drug particle and a substrate surface can be determined (11).

In the absence of any significant electrostatic force or upon complete dissipation of the build-up of electrostatic charges from interacting surfaces, the principal forces contributing to particle adhesion are the van der Waals and capillary forces. Various theoretical models, derived from the Hertz approximation (12), have been developed to determine the van der Waals force of interaction. The two most commonly used models are the Johnson-Kendall-Roberts (JKR) (13) and the Deryaguin-Muller-Toporov (DMT) (14) models. The resulting force of adhesion between two spheres is provided in equation (1):

$$F_{vdw} = n\pi R^* W_{ad} \tag{1}$$

where R* is the harmonic mean of the particle radii (also called contact radius), W_{ad} is the thermodynamic work of adhesion ($mJ \cdot m^{-2}$), and n is a predetermined constant depending on the selected model (n = 3/2 for JKR and n = 2 for the DMT).

Capillary forces arise from the dynamic condensation of water molecules onto particle surfaces. If the amount of condensed water is sufficient, a meniscus is formed between the contact points of the adjacent surfaces as liquid is drawn by capillary action around the contact points, inducing an attractive force. Fisher and Israelachvili (15) proposed a method to predict the capillary interaction between two spherical particles. The subsequent capillary force equation is shown below:

$$F_c = 4\pi R^* \gamma_L \cos\sigma + 4\pi R^* \gamma_{SL} \tag{2}$$

Where γ_L is the water surface tension, γ_{SL} is the solid-liquid interfacial free energy, and θ is the measured contact angle of the liquid with the particle surface.

It should be highlighted that both the thermodynamic work of adhesion W_{ad} and contact angle are directly dependant on the surface free energies and the interfacial free energy of the interacting surfaces. Furthermore, van der Waals and capillary forces are directly proportional to particle radii (i.e., contact area). Thus, these two factors are of critical importance in the quantification of interparticle forces.

Measurements of the pull-off forces between pharmaceutical particles with irregular morphologies and varying degree of surface roughness have previously been reported (16). Although the effects of surface roughness on variations in adhesion forces are acknowledged, direct quantification of true contact area between two contiguous surfaces remains difficult (7). More recently, however, a method for characterising the contact area between a micronized particle and a substrate surface has been developed (17,18). This AFM based approach involves scanning a colloidal drug probe over a grid composed of very sharp asperities. Due to a limitation in the Villarrubia algorithm utilized to reconstruct the substrate topography, a reverse surface image of the tip is recorded. Although an estimate of the area of contact of a micron sized

[1] Pharmaceutical Technology Research Group, Department of Pharmacy & Pharmacology, University of Bath Bath, BA2 7AY, UK.
[2] Vectura Ltd, Chippenham, SN14 6FH, UK.
[3] To whom correspondence should be addressed. (e-mail: r.price@bath.ac.uk)

particle can subsequently be discerned, the approach is limited when considering the surface deformation of the interacting materials and the variations between two substrate surfaces of different rugosities.

Model substrate surfaces for AFM colloid probe investigations are commonly prepared by high-pressure compaction tableting (17,19). It is speculated that the high loading pressures required are sufficient to induce local defects and dislocations, and potentially significant areas of amorphous disorder (20,21). The presence of these amorphous domains may alter the surface free energy properties of the substrate material and subsequently modify the associated mechanical properties and thermodynamic work of cohesion/adhesion upon interaction.

In this study, model drug and carrier particles were crystallized directly from solution to obtain well-defined and highly reproducible single crystals with characteristically smooth and planar surfaces. Although the contact area between an interacting probe and substrate would remain unknown, the uniform texture of substrate surfaces should allow direct comparison of interactions between a specific colloid probe and an array of substrate materials. This AFM based approach may provide a novel means of quantifying the cohesive and adhesive interactions within a dry powder formulation and ultimately provide a critical understanding of the force balance, which directly influence the overall characteristics and performance of a dry powder formulation.

MATERIALS AND METHODS

Materials

Budesonide was supplied from Sicor (Batch number 6157/MI, Santhia, Italy), salbutamol sulfate from Becpharm Ltd (Batch number 940077, London, UK) and Sorbalac 400 lactose from Meggle (Wasserburg, Germany). All were used as supplied. Methanol was HPLC grade (Fisher Chemicals, Loughborough, UK. AnalaR grade ethanol and acetic glacial were supplied by BDH (Poole, UK). Ultra pure water was produced by reverse osmosis (MilliQ, Millipore, Molsheim, France).

Crystallization of Substrate Materials

Saturated solutions of budesonide in ethanol, salbutamol sulfate in water and lactose in water were prepared prior to recrystallization. Samples were shaken for 12 h at 20°C (G76, Gyrotory water bath shaker, New Brunswick Scientific, Edison, NJ, USA) in sealed volumetric flasks prior to filtration via a 0.22-μm membrane filter (Whatman Inc., Clifton, NJ, USA).

Budesonide, salbutamol sulfate and lactose were crystallized by primary nucleation, using an anti-solvent as a precipitating agent. A schematic representation of the crystallization apparatus is shown in Fig. 1. A microscope cover slip (12 mm × 12 mm) was supported on a vertical post in a crystallization dish, which contained the anti-solvent (water for budesonide, ethanol for both lactose and salbutamol sulfate). A droplet (~1 ml) of the saturated solution was placed on the cover slip via a glass pipette. The system was sealed by inverting a suitable glass beaker in the crystallization dish. Upon equilibration of the vapor phases of the miscible solvents, nucleation and crystal growth within the solution droplet occurred. The glass cover slip was subsequently removed and fixed onto a magnetic stub with glass bond glue (Loctite, Welwyn City, UK) for AFM studies. The heterogeneous nucleation and growth of the crystals onto the glass cover slips precluded the need for any sample preparation of the crystals for AFM investigations.

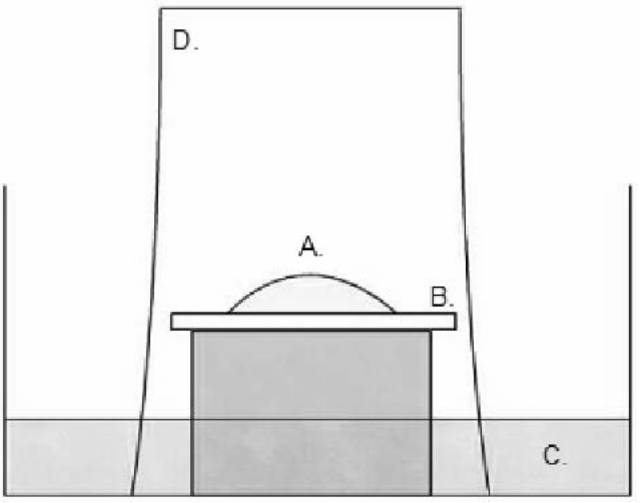

Fig. 1. Schematic representation of the anti-solvent recrystallization step: (A) saturated solution droplet, (B) glass slide, (C) crystalline dish containing the anti-solvent, (D) beaker.

Scanning Electron Microscopy

The morphology of the single crystals of budesonide, salbutamol sulfate and lactose were investigated using a scanning electron microscope (SEM) (Jeol 6310, Jeol, Tokyo, Japan). Samples were gold-coated (Edwards Sputter Coater, Crawley, UK) prior to imaging.

Computer Simulation of Crystal Habits

The Miller indices of the dominant growth faces of the crystals obtained were identified using a 3D simulation program (SHAPE V7.0, Shape Software, Kingsport, Tennessee, USA). The 3D crystal structures required the input of the unit cell lattice parameters and the space group symmetry operators. Budesonide crystallizes in the orthorhombic crystal system (a = 8.550 Å, b = 9.406 Å, and c = 28.401 Å), space group $P2_12_12_1$ (22). Salbutamol sulfate crystallizes in the monoclinic crystal system, (a = 28.069 Å, b = 6.183 Å, c = 16.914 Å and β = 81.19°), space group C_c (23). Alpha-lactose monohydrate crystallizes in the monoclinic crystal system (a = 7.982 Å, b = 21.562 Å, c = 4.824 Å and β = 109.57), space group $P2_1$ (24).

Atomic Force Microscopy (Topography)

The surface topography and roughness measurements of budesonide, salbutamol sulfate and lactose crystals were investigated using a Nanoscope IIIa controller, a Multimode AFM and a J-type scanner (DI, Santa Barbara, CA, USA). All AFM surface topography images were recorded in Tapping Mode operation (TM-AFM). Tetrahedral-tipped silicon-etched cantilevers (OTSP, Digital Instruments) were used for

imaging. Surface roughness measurements were analyzed over a 2.5 μm × 2.5 μm area. To quantify the variations in the surface properties of the crystal surfaces, the root-mean-squared surface roughness measurement (R_q) and the mean surface roughness (R_a) of the height deviations of the surface asperities were computed.

Atomic Force Microscopy (Interaction Force Measurements)

Prior to force measurements, particles (n = 3 for each material) of budesonide, salbutamol sulfate and lactose were fixed onto standard V-shaped tipless cantilevers (DNP-020, Digital Instruments, CA, USA) using an epoxy resin glue (Araldite, Cambridge, UK). The spring constant (k) of the cantilevers was determined by the thermal noise method (k = 0.282 ± 0.039 N/m). The preparation of these colloid probes has been described in detail elsewhere (7).

The AFM was housed in an environmental chamber and the ambient conditions maintained at a constant temperature of 25°C (±0.2°C) and relative humidity of 35% RH (±3%), The partial water vapor pressure was controlled via a custom-built perfusion unit coupled to a highly sensitive humidity sensor (Rotronic AG, CH). The interaction forces were measured by recording the deflection of the AFM cantilever as a function of the substrate displacement (z) by applying Hooke's law (F = −kz). Individual force curves (n = 4096) were conducted over a 2.5 μm × 2.5 μm at a scan rate of 4 Hz and a compressive loading of 40 nN. These parameters were kept constant throughout the study. Statistical analysis of these data was performed by Fisher's pairwise comparison of one-way ANOVA with 99% confidence limits.

RESULTS

In order to gain a fundamental insight into the interactive forces which govern the interactive mixing and aerosol delivery characteristics of a dry powder formulation, the relative cohesive-adhesive balances need to be quantified within such systems. In this study, an equivalent contact geometry approach was utilized to determine the force balances within model dry powder inhalation formulations. The cohesion and adhesion properties of micron sized budesonide, salbutamol sulfate and lactose probes were investigated using an AFM colloid probe technique.

Scanning Electron Microscopy

Representative scanning electron micrographs and simulated morphologies of the dominant growth faces of crystallized budesonide, salbutamol sulfate and lactose are shown in Figs. 2A, 2B, and 2C and Fig. 2A_α, B_α, and C_α, respectively. Budesonide crystals displayed an elongated dodecahedral shape in relation to the growth of the dominant $(01\bar{2})$ and $(0\bar{1}\bar{2})$ Miller indices. Electron micrographs of salbutamol sulfate crystals suggested a needle like morphology dominated by the (200) face, while the majority of lactose crystals exhibited the well-known tomahawk shape, dominated by the (100) and $(1\bar{1}0)$ crystalline faces. The single crystals exhibited highly smooth surface textures.

Atomic Force Microscopy (Topography)

Representative AFM amplitude images of the dominant single crystal faces of budesonide, salbutamol sulfate and

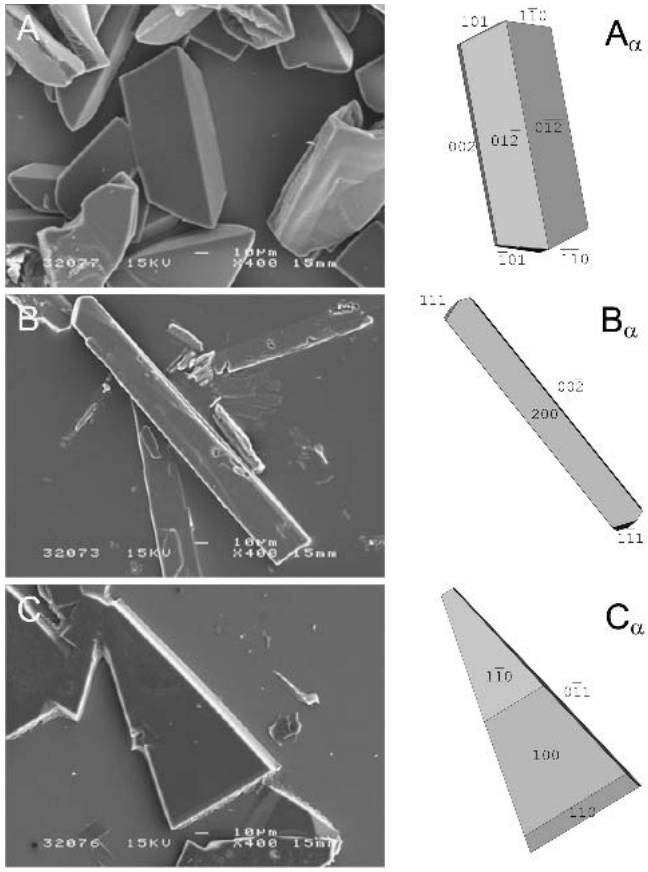

Fig. 2. Representative SEM images and corresponding simulated morphologies (α) of recrystallized budesonide (A), salbutamol sulfate (B), and α-lactose monohydrate (C).

α-lactose monohydrate are shown in Figs. 3A, 3B, and 3C, respectively. Topographical AFM images indicated varying degrees of nanometre roughness for the model substrate surfaces. These variations were probably related to differing growth processes and kinetics during crystallization. The surface rugosity R_a (average height from the center line) and root mean square deviation R_q (variability of the profile from the center line) of the three samples are shown in Table I. The data confirmed the extremely smooth surface morphology of the crystals faces observed by SEM, exhibiting surface roughness measurements well below 5 nm. It should be noted that there was no observable modification in surface morphology over large areas (>20 μm^2) of the crystal faces. Thus, the engineered crystal substrates should provide highly suitable surfaces for quantitative analysis of the force balance in model dry powder formulations.

Interaction Force Measurements by Atomic Force Microscopy

The mean adhesive/cohesive forces of the interaction of a series of budesonide, lactose and salbutamol sulfate colloid probes and engineered substrate surfaces are shown in Figs. 4, 5, and 6, respectively. For consistency, the dominant crystal face of each material was chosen and care was taken to place the probes in the same region on the substrate for each experiment. For all systems, the force distributions could be fitted to a Gaussian distribution, related to the uniformity in

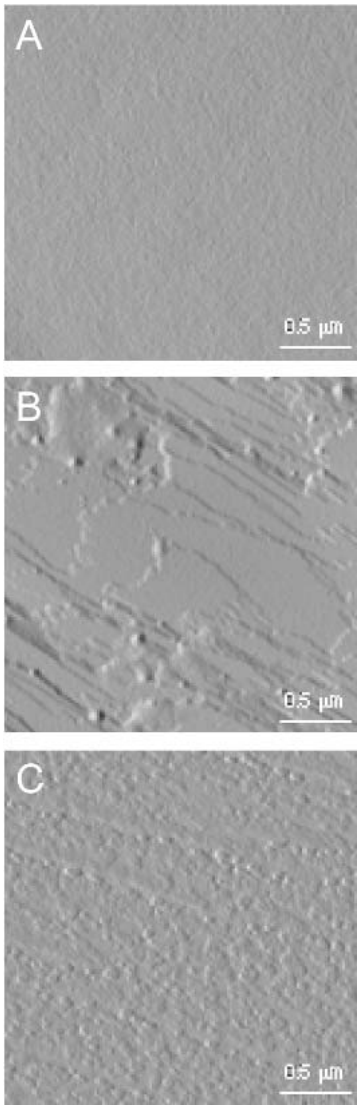

Fig. 3. Representative AFM amplitude images of the surface of recrystallized budesonide (A), salbutamol sulfate (B), and α-lactose monohydrate (C).

contact area between probe and multiple contact points on the substrate surface. Furthermore, the small standard deviation of the distributions confirmed the suitability of the engineered crystal surfaces in producing highly accurate and reproducible data.

Since the drug probes were prepared from untreated material, variability in probe geometry was expected. This would result in significant variations in contact area between each probe and the model substrate surface and concomitantly the adhesion force measurements. This variation in contact geometry was highlighted by the variations in adhesion force measurements between each probe and a given substrate. Nevertheless, a relationship between adhesive and cohesive interactions could be obtained by determining the specific variation in interaction between each individual probe and model substrate surfaces.

Table I. Roughness Properties of Budesonide, Salbutamol Sulfate, and α-Lactose Monohydrate

	Budesonide	Salbutamol sulfate	α-Lactose monohydrate
Rugosity (nm)	0.681	2.258	1.837
RMS (nm)	0.872	3.142	2.284

The adhesion force of interaction between a series of budesonide probes and α-lactose monohydrate, salbutamol sulfate and budesonide crystal substrates are shown in Fig. 4. The adhesive interaction between budesonide and lactose were significantly higher than with salbutamol sulfate ($p < 0.01$). However, a significant increase and overall dominance of the cohesive interaction was observed for all budesonide probes ($p < 0.01$).

Interaction forces between salbutamol sulfate probes and the dominant crystal faces of α-lactose monohydrate, salbutamol sulfate and budesonide crystal substrates are shown in Fig. 5. In contrast to budesonide interactions, the salbutamol sulfate probes exhibited extremely weak cohesive properties with respect to the adhesive interactions with both α-lactose monohydrate and budesonide ($p < 0.01$). The adhesive interactions between salbutamol sulfate and lactose were significantly higher than the adhesive salbutamol sulfate-budesonide interaction ($p < 0.01$).

Interaction forces between lactose probes and α-lactose monohydrate, salbutamol sulfate and budesonide crystal substrates are illustrated in Fig. 6. The adhesive interaction between a lactose and salbutamol sulfate were significantly greater than both the cohesive lactose-lactose and adhesive lactose-budesonide interaction ($p < 0.01$). However, the cohesive lactose interactions were significantly greater than the adhesive interactions between lactose and budesonide ($p < 0.01$).

It is interesting to note that the balance of forces for the budesonide, salbutamol sulfate and lactose probes differed significantly.

DISCUSSION

The balance of interparticulate forces within dry powder inhaler formulations is critical in the mixing, de-aggregation and dispersion properties of active pharmaceutical ingredients. However, quantitative measurements of these funda-

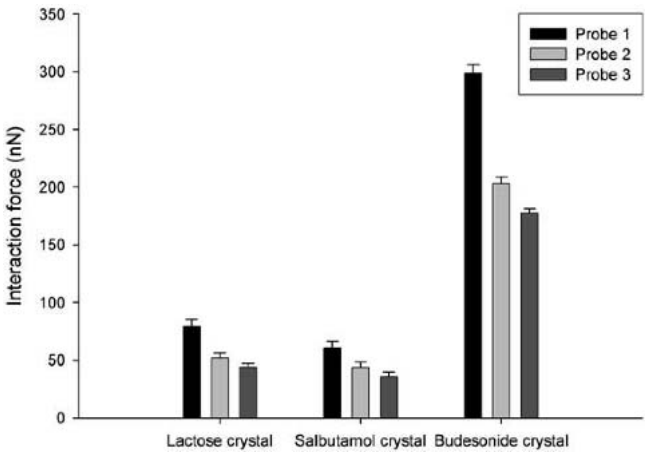

Fig. 4. Interaction forces between budesonide probes and α-lactose monohydrate, salbutamol sulfate, and budesonide crystal substrates.

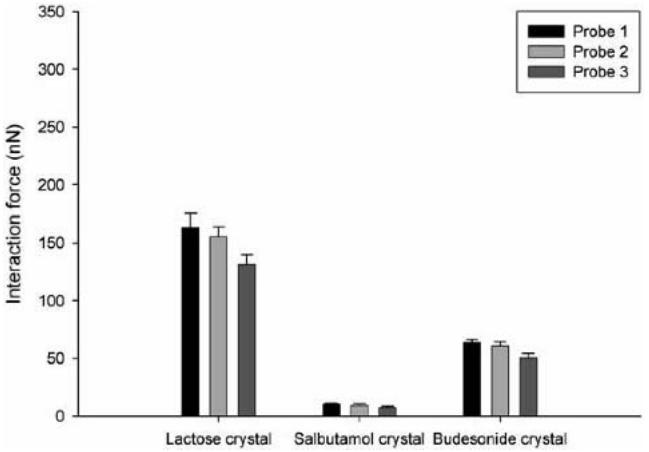

Fig. 5. Interaction forces between salbutamol sulfate probes and α-lactose monohydrate, salbutamol sulfate, and budesonide crystal substrates.

mental interactions and their specific role on blending and aerosolization behavior have not been fully realized. Such measurements have been limited due to the complex nature of the physico-mechanical interactions and, in particular, the major influence of variations in contact area on particle adhesion. Furthermore, efforts to predict the adhesion forces using theoretical approaches and surface energy measurements have proven unsatisfactory (25,26). Theoretical estimates are often several orders of magnitude greater than experimental measurements. The most plausible explanation for this disparity is that the true contact area between contiguous surfaces is significantly less than expected macroscopic dimensions.

In this study, a novel analysis of the AFM colloid probe technique has been utilized to determine the cohesive-adhesive force balances within model dry powder formulations. Controlling the nanoscale morphology of dominant growth faces of drug and excipient crystals substantially reduced the influence of substrate surface roughness on particle adhesion, as described previously (7). Under controlled environmental conditions, force measurements were observed to be highly reproducible. However, quantification of force measurements was precluded, as it would require normalization through the determination of the probe-substrate contact area.

In order to overcome these limitations, the ratios of adhesive and cohesive balances were compared rather than the separation forces. From theory, this cohesive-adhesive balance between materials A and B can be expressed as:

$$\frac{F_{A-A}}{F_{A-B}} = \frac{R^*_{A-A}[n\pi W_{A\text{-}A} + (4\pi\gamma_{water}\cos\theta_{A\text{-}A} + 4\pi\gamma_{A\text{-}water})]}{R^*_{A-B}[n\pi W_{A\text{-}B} + (4\pi\gamma_{water}\cos\theta_{A\text{-}B} + 4\pi\gamma_{A\text{-}water})]} \quad (3)$$

where $F_{A\text{-}A}$ and $F_{A\text{-}B}$ are the cohesive and adhesive forces, respectively. It can be concluded from Eq. 3 that with constant environmental conditions, the work of adhesion and contact angle are only dependant on the material physical characteristics. For a colloidal particle interacting with the substrate materials, the only parameters which are susceptible to vary are the contact radii R^*_{A-A} and R^*_{B-B}. Assuming the similarity of the two tailored substrate surface contact radii, the cohesion-adhesion ratios for a number of interacting probes of a specific material should theoretically remain constant. Thus, by plotting the measured force of cohesion as a function of the force of adhesion for a number of probes, the force balance within a model formulation could be quantified.

A cohesive-adhesive balance (CAB) graph of a theoretical binary system is illustrated in Fig. 7. The adhesive force measurements for a number of probes of the interacting materials (F_{A-B} and F_{B-A}) are plotted on the x-axis; the related forces of cohesion (F_{A-A} and F_{B-B}) of the respective probes are plotted on the y-axis. For equivalent contact geometry, the force data of several probes of a specific material plotted on a CAB-graph should follow a linear fit, resulting from the consistency in the cohesive-adhesive balance ratio (F_{A-A}/F_{A-B}) and (F_{B-B}/F_{B-A}). The bisecting line corresponds to equilibrium between forces of adhesion and forces of cohesion, which defines two distinctive regions. The relative position of the aligned plots with respect to the bisector is a direct indication of the cohesive-adhesive balance of the interacting material within the binary system. As indicated, plots in the lower section indicate an affinity for the probe material to develop adhesive interactions ($F_{adh.} > F_{coh.}$). Conversely, plots in the upper section of the graph denote a dominancy of cohesive properties. Quantitative information regarding the

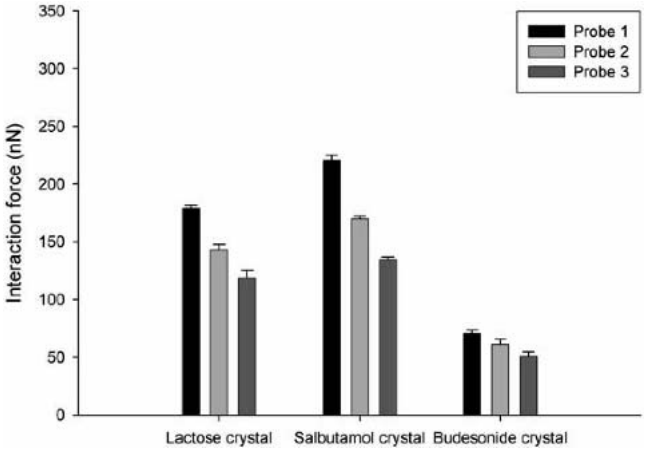

Fig. 6. Interaction forces between lactose probes and α-lactose monohydrate, salbutamol sulfate, and budesonide crystal substrates.

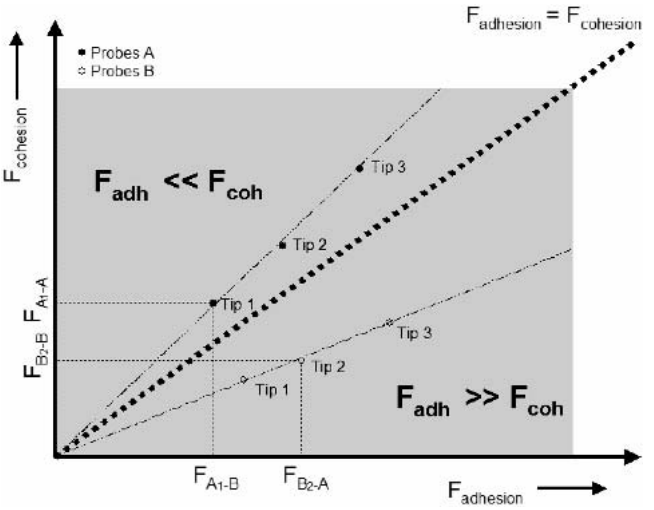

Fig. 7. Description of a CAB-graph for a theoretical binary system.

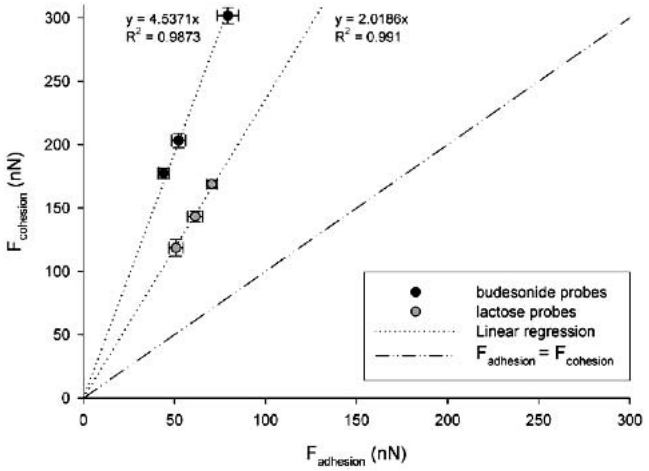

Fig. 8. Comparison between forces of adhesion and force of adhesion in a binary lactose/budesonide system.

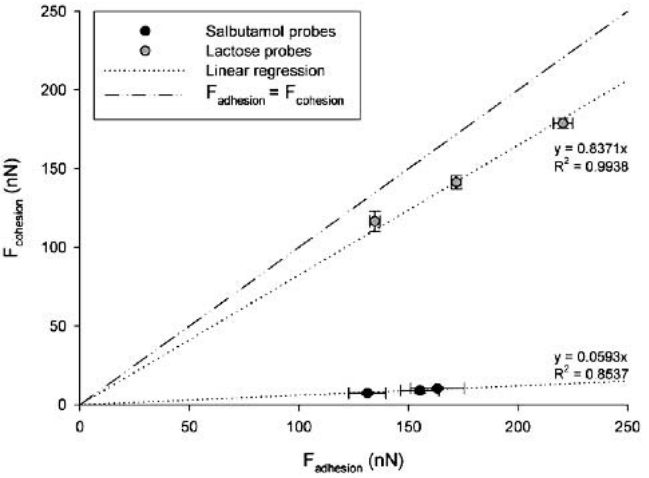

Fig. 9. Comparison between forces of adhesion and force of adhesion in a binary lactose/salbutamol sulfate system.

relative strength of the adhesive/cohesive interactions can be directly measured by the relative slope of the linear regression.

From the force measurements in Fig. 4, a CAB-graph of a lactose-budesonide system is shown in Fig. 8. A linear regression was performed for each set of data to verify the consistency of contact area uniformity of probe interaction from one substrate to another. A coefficient of determination (R^2) of 0.9910 and 0.9873 for the lactose probes and budesonide probes, respectively, confirmed uniformity in contact area between crystals and the relationship between adhesion and cohesion for the interactive probes. Furthermore, the two plots indicated that for an equivalent contact area, both budesonide and lactose particles experience a greater affinity for cohesive interactions. The measurement of the relative slopes suggested that the budesonide-budesonide interactions are 3.84-fold greater than the adhesive budesonide-lactose interactions, while lactose-lactose interactions are 2.36-fold greater than the adhesive lactose-budesonide interactions. From a formulation perspective, the data suggested that this binary system would exhibit poor blend homogeneity unless a significant amount of shear energy was introduced to overcome the cohesive bonds. Moreover, such a formulation would possibly be subjected to segregation over time due to the very strong budesonide cohesive bonds.

A CAB-graph generated from the data in Fig. 5 for a lactose-salbutamol sulfate system is shown in Fig. 9. The linearity of the data was again validated, with a coefficient of determination of 0.9938 and 0.8537 for the lactose probes and salbutamol sulfate probes, respectively. The relative position of the data below the bisecting line indicated the two materials possess a strong affinity for one another with respect to their cohesive interactions (particularly salbutamol sulfate). The measurement of the slopes indicated that the interaction between salbutamol sulfate and lactose is 16.88 times and 1.22 times greater than the cohesive salbutamol sulfate and lactose interactions, respectively. Upon processing such a powder formulation, the system should not require an excessive amount of energy to generate a homogenous blend with good content uniformity.

The novel treatment of the AFM data has provided a potentially useful technique in the quantitative determination of the force balance within binary systems. This process, however, may be further expanded to more complex formulations, for example, combination product formulations, by cross normalising the data. The resulting cohesive-adhesive balance dependencies between salbutamol sulfate, lactose and budesonide are summarized in Table II. The cohesive salbutamol sulfate interactions ratio was set to 1.00 and all the subsequent CAB ratios were calculated relative to this reference ratio. The corresponding matrix provides a complete description of all the various interaction forces within a ternary system. Furthermore, cross normalization provides a novel means of measuring the hierarchy of the cohesive forces of the materials. The coefficient of proportionality with respect to salbutamol sulfate for lactose and budesonide is 14.13 and 31.76, respectively.

CONCLUSIONS

The colloid probe AFM technique has been utilized to measure the characteristics of the inter-particulate forces that govern bulk properties of dry powder formulations. The tailoring of well-defined substrate surfaces minimized intravariations in contact area of a colloid probe. This enabled direct characterization of the adhesive and cohesive interactions within a model dry powder inhaler formulation. Together with the development of a novel cohesive-adhesive balance (CAB) analysis procedure, a quantitative relationship between measurements of the relative interactions within

Table II. Cohesive-Adhesive Balance Dependency Between Salbutamol Sulfate, Lactose, and Budesonide Interaction Combinations

	CAB dependency		
Sample	Salbutamol sulfate†	α-Lactose monohydrate†	Budesonide†
Salbutamol sulfate*	1.00 ± 0.08	16.88‡ ± 0.85	6.59‡ ± 0.00
Lactose*	16.88‡ ± 1.06	14.13‡ ± 1.06	7.00‡ ± 1.6
Budesonide*	6.59‡ ± 0.32	7.00‡ ± 1.6	31.76‡ ± 1.53

* Probe.
† Substrate.
‡ $p < 0.01$.

dry powder inhaler formulations was achievable. In combination with bulk techniques, this novel approach may provide a pivotal role in predicting blending, segregation and dispersion characteristics of active pharmaceutical ingredients in dry powder systems.

REFERENCES

1. W. C. Hinds. *Aerosol technology: Properties, Behaviour and Measurements of Airborne Particles*, Wiley, New York, 1999.
2. N. M. Ahfat, G. Buckton, R. Burrows, and M. D. Ticehurst. Predicting mixing performance using surface energy measurements. *Int. J. Pharm.* **156**:89–95 (1997).
3. D. Cline and R. Dalby. Predicting the quality of powders for inhalation from surface energy and area. *Pharm. Res.* **19**:1274–1277 (2002).
4. G. Buckton. Characterisation of small changes in the physical properties of powders of significance for dry powder inhaler formulations. *Adv. Drug Deliv. Rev.* **26**:17–27 (1997).
5. R. N. Jashnani, P. R. Byron, and R. N. Dalby. Testing of Dry Powder Aerosol Formulations in Different Environmental-Conditions. *Int. J. Pharm.* **113**:123–130 (1995).
6. V. Berard, E. Lesniewska, C. Andres, D. Pertuy, C. Laroche, and Y. Pourcelot. Dry powder inhaler: influence of humidity on topology and adhesion studied by AFM. *Int. J. Pharm.* **232**:213–224 (2002).
7. R. Price, P. M. Young, S. Edge, and J. N. Staniforth. The influence of relative humidity on particulate interactions in carrier-based dry powder inhaler formulations. *Int. J. Pharm.* **246**:47–59 (2002).
8. M. C. Korecki and P. J. Stewart. Adhesion of solid particles to solid surface. *A.M.A. Arch. Env. Health* **1**:13–21 (1987).
9. J. N. Staniforth, J. E. Rees, F. K. Lai, and J. A. Hersey. Determination of interparticluate forces in ordered powder mixes. *J. Pharm. Pharmacol.* **33**:485–490 (1981).
10. M. E. Mullin, L. P. Michaels, V. Menon, B. Locke, and M. B. Ranade. Effect of geometry on particle adhesion. *Aerosol Sci. Tech.* **17**:105–118 (1992).
11. W. A. Ducker, T. J. Senden, and R. M. Pashley. Direct Measurement of Colloidal Forces Using an Atomic Force Microscope. *Nature* **353**:239–241 (1991).
12. H. Hertz. Study on the contact of elastic solid bodies (SLA translations, SLA-57-1164). *Zeitschr. F. Reine Angewandte Mathehmatik* **29**:156–171 (1881).
13. K. L. Jonhson, K. Kendall, and A. D. Roberts. Surface energy and the contact of elastic solids. *Proc. Roy. Soc. London* **324**:301–303 (1971).
14. B. V. Deryaguin, V. M. Müller, and Y. P. Toporov. Effect of contact deformations on the adhesion of particles. *J. Colloid Interface Sci.* **53**:314–325 (1975).
15. L. R. Fisher and J. N. Israelachvili. Direct measurements of the effect of meniscus forces on adhesion: a study of the applicability of macroscopic thermodynamics to microscopic surfaces. *Colloids and Surfaces* **3**:303–319 (1981).
16. E. R. Beach, G. W. Tormoen, J. Drelich, and R. Han. Pull-off force measurements between rough surfaces by atomic force microscopy. *J. Colloid Interface Sci.* **247**:84–99 (2002).
17. U. Sindel and I. Zimmermann. Measurement of interaction forces between individual powder particles using an atomic force microscope. *Powder Technol.* **117**:247–254 (2001).
18. J. C. Hooton, C. S. German, S. Allen, M. C. Davies, C. J. Roberts, S. J. B. Tendler, and P. M. Williams. Characterization of particle-interactions by atomic force microscopy: Effect of contact area. *Pharm. Res.* **20**:508–514 (2003).
19. P. G. Royall, D. Q. M. Craig, D. M. Price, M. Reading, and T. J. Lever. An investigation into the use of micro-thermal analysis for the solid state characterisation of an HPMC tablet formulation. *Int. J. Pharm.* **192**:97–103 (1999).
20. L. Mackin, R. Zanon, J. M. Park, K. Foster, H. Opalenik, and M. Demonte. Quantification of low levels (<10%) of amorphous content in micronised active batches using dynamic vapour sorption and isothermal microcalorimetry. *Int. J. Pharm.* **231**:227–236 (2002).
21. P. Begat, P. M. Young, S. Edge, J. S. Kaerger, and R. Price. The effect of mechanical processing on surface stability of pharmaceutical powders: Visualization by atomic force microscopy. *J. Pharm. Sci.* **92**:611–620 (2003).
22. J. Albertsson, A. Oskarrson, and C. Svensson. X-ray Study of Budesonide: molecular structure and solid solution. *Acta Crystallogr.* **B34**:3027–3036 (1978).
23. J.-M. Leger, M. Goursolle, and M. Gadret. Structure Cristalline du Sulfate de Salbutamol [tert-butylamino-2 (Hydroxy-4hydroxymethyl-3 phenyl)-1 Ethanol. 1/2 H2SO4. *Acta Crystallogr.* **B34**: 1203–1208 (1978).
24. M. Kurimoto, P. Subramony, and R. W. Gurney. Kinetic Stabilization of Biopolymers in Single-Crystal Hosts: green fluorescent Protein in Alpha-Lactose monohydrate. *J. Am. Chem. Soc.* **121**: 6952–6953 (1999).
25. D. M. Schaefer, M. Carpenter, R. Reifenberger, L. P. Demejo, and D. S. Rimai. Surface Force Interactions between Micrometer-Size Polystyrene Spheres and Silicon Substrates Using Atomic-Force Techniques. *J. Adhes. Sci. Technol.* **8**:197–210 (1994).
26. D. M. Schaefer, M. Carpenter, B. Gady, R. Reifenberger, L. P. Demejo, and D. S. Rimai. Surface-Roughness and Its Influence on Particle Adhesion Using Atomic-Force Techniques. *J. Adhes. Sci. Technol.* **9**:1049–1062 (1995).